Design of a compact synchrotron for medical applications

Nader Al Harbi and S. Y. Lee[a)]
Department of Physics, Indiana University, Bloomington, Indiana 47405

(Received 3 October 2002; accepted 26 January 2003)

An optimal design of a low energy (300 MeV) proton synchrotron for medical applications is addressed. The machine has the following properties: (1) The transition energy is higher than the targets final proton beam energy of 300 MeV; (2) the betatron tunes are chosen such that the machine is free of systematic resonances; (3) the machine can accommodate both slow and fast extraction systems; and (4) the machine can provide rapid cycling operations depending on the rf cavity voltage. Applications of this low energy synchrotron are discussed. © *2003 American Institute of Physics.* [DOI: 10.1063/1.1561598]

I. INTRODUCTION

In recent years, particle beams have often been used in the production of isotopes for nuclear medicine, radiation therapy and surgery, ion doping, nanotechnology, and industrial processing. For proton beam cancer therapy, it is usually argued that the preferred energy of a proton beam should be able to vary from 70 to 300 MeV.[1] This requirement can best be fulfilled by employing a synchrotron type of accelerator design.

Existing proton accelerators for radiation treatment include the Loma Linda proton synchrotron, Massachusetts General Hospital (MGH) proton cyclotron, a 200 MeV cyclotron and a 220 MeV proton synchrotron at the Midwest Proton Radiation Institute (MPRI) at the Indiana University Cyclotron Facility (IUCF), and others.[2] Although there have been great advancements in the design of proton cyclotrons in areas such as compactness and beam intensity, the cyclotron is still limited by its size at higher energies, flexibility in its beam delivery system, and variation in beam energy. This article is intended to provide an optimal design for a medical synchrotron with a maximum energy of 300 MeV.

There have been many attempts to design efficient, low energy proton synchrotrons for medical applications in the past few years.[3] The energy of these accelerators is usually slightly too low, and the straight sections of these designs are too short to accommodate both slow and fast extraction systems. Difficulties in the design of low energy synchrotrons are (1) the complication in transition energy crossing, (2) the availability of both slow and fast extractions, (3) space charge effects, and (4) control of the beam intensity. For example, the low energy proton synchrotron at the Loma Linda Medical Center utilizes the weak focusing principle so that the beam is always above the transition energy, where $\gamma_T \leqslant 1$ for a weak focusing synchrotron, while the Cooler Injector Synchrotron (CIS) at the IUCF is limited to a proton beam energy of about 220 MeV.

This article addresses the above design hurdles and finds a solution for proton accelerators with a maximum proton energy of 300 MeV. Our design is based on the principle of minimizing the number of accelerator components so that a flexible control system can easily be implemented at minimum cost. Following the successful construction of the CIS at the IUCF,[4] we design our compact medical synchrotron (CMS) using a similar configuration. The accelerator is composed of four dipoles, a charge exchange injection section, a rf accelerating system, and slow and fast beam extraction systems. We organize our paper as follows. Section II lists characteristic parameters of the accelerator and discusses the design concept. Section III discusses the design of a simple C-shaped dipole magnet, its nonlinear magnet multipoles, and dynamical aperture. Section IV describes the requirements for a rf system. Section V illustrates the injection and extraction scenarios. A discussion of the implementation of this synchrotron is given in Sec. VI.

II. BASIC PARAMETERS

A wish list for a low energy proton synchrotron for medical applications can be written as follows.

(1) The proton energy should be easily varied from 70 to 300 MeV. During acceleration, the bunched beam should avoid crossing the transition energy. The beam energy preferably should be below the transition energy in order to avoid negative mass instability.
(2) The beam intensity should be higher than 2×10^{11} particles per pulse.
(3) The synchrotron should have the capability to perform both fast and slow extractions, i.e., the betatron tunes should be chosen to facilitate this capability.

The layout of a Compact Medical Synchrotron (CMS) that meets these requirements is shown in Fig. 1. The machine parameters are listed in Table I. We now examine solutions in achieving the parameters listed.

A. Space charge and beam intensity

The performance of low energy synchrotrons is limited essentially by space charge force, characterized by the incoherent space charge betatron detuning parameter:[5,6]

a)Electronic mail: shylee@indiana.edu

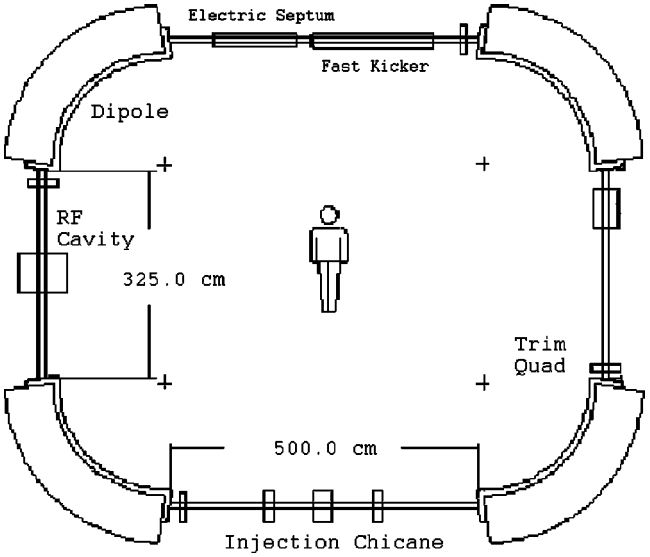

FIG. 1. Schematic of the layout of the compact medical synchrotron. The lengths of the straight sections are $a=5.00$ m and $b=3.25$ m. The length of each dipole is 3.00 m. The total circumference is 28.5 m.

$$\Delta\nu_{\mathrm{sc}}=\frac{F_{\mathrm{dist}}F_B N_B r_0}{2\pi\beta^2\gamma^3\epsilon}, \tag{1}$$

where F_{dist} is the density factor that depends on the transverse distribution of the beam, $F_B=C/(\sqrt{2\pi}\sigma_\ell)$ is the bunching factor, C is the circumference of the accelerator, σ_ℓ is the root mean square (rms) bunch length, N_B is the number of particles in a bunch, r_0 is the classic radius of the charged particle, and ϵ is the beam emittance. Typical values of the space charge betatron detuning parameter in low energy synchrotrons hover around 0.25. This number can be easily dealt with by choosing appropriate beam parameters and the appropriate injection energy.[5] A typical injector is composed of a H^- ion source and a radio-frequency quadrupole (RFQ) and accelerator and a drift-tube linac (DTL) for charge-strip injection into the synchrotron. To attain $N_B \approx 2.1\times10^{11}$ particle per pulse, we find that the minimum injection energy is 7 MeV for a source intensity of at least 1 mA and 100 turn accumulation in the synchrotron. At a higher injection energy, the beam brightness of the synchrotron can be raised.[7] The design can deliver an average current of about 0.5 μA at a 15 Hz ramping rate, or 33 nA at a 1 Hz ramping rate. The resulting beam emittance depends on the injection process, the space charge effect, and the dynamical aperture of the synchrotron.

TABLE I. List of parameters of low energy proton synchrotrons.

Parameter	CMS	CIS	Loma Linda
Circumference C (m)	28.5	17.6	20.0476
Bending radius ρ (m)	1.909 86	1.273	1.6
Dipole edge angle (deg)	8.5	12	18.8
Injection energy, E_{inj} (MeV)	7–10	7	2
Extraction energy E_{max} (MeV)	10–300	7–220	70–250
$\hat{\beta}_x/\hat{\beta}_y/\hat{D}$ (m)	10.4/7.8/2.4	4.4/3.8/1.8	6.1/2.8/9.6
ν_x/ν_z	1.6825/0.6838	1.45/0.78	0.600/1.356
C_x/C_z	$-1.14/-0.18$	$-0.53/-0.16$	0.88/0.36
γ_T	1.393	1.271	0.578
N_B	2.1×10^{11}	1.0×10^{11}	1.0×10^{11}
ϵ_x/ϵ_z (π mm mrad)	100/100	100/100	100/100

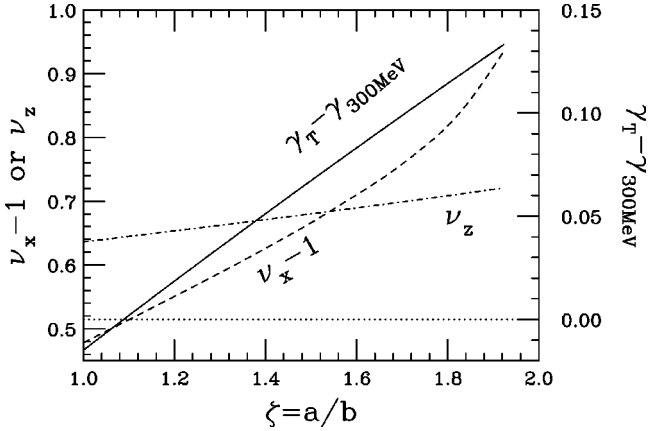

FIG. 2. Betatron tunes Q_x-1 and Q_z, and the transition $\gamma_T-\gamma_{(300\ \mathrm{MeV})}$ are shown as functions of the drift space ratio $\zeta=a/b$. Note that $\gamma_T\sim\sqrt{Q_x}$, γ_T depends nearly linearly on ζ, and there is an integer stopband at $\zeta\approx1.93$.

Once the basic machine parameters are established, the task is to design an optimized machine lattice in which the beam is accelerated to the desired energy. We prefer a simple machine with four 90° dipoles, where a strong horizontal focusing arises from the bending radius of dipole magnets and vertical focusing from the dipole edge angle. For a lattice with four fold symmetry, the transition energy lies below the maximum beam energy of 300 MeV.[4] Thus we choose a racetrack-like accelerator layout like ($D1\ B\ D2\ B$), where B stands for the dipole, and $D1$ and $D2$ are drift spaces with lengths a and b, respectively (see Fig. 1).

B. Transition energy consideration

Figure 2 shows the betatron tunes ν_x-1 and ν_z, and transition energy $\gamma_T-\gamma_{(300\ \mathrm{MeV})}$, as a function of the ratio of the lengths of the long and short straight sections ($\zeta=a/b$), where we choose $b=3.25$ m and a dipole edge angle of 8.5° for edge focusing. The length of 3.25 m is chosen so that there is enough free space for the beam extraction septum and clearance of the beam extraction channel. From Fig. 2, we note that if we keep $a/b\geqslant1.1$, the beam energy will be below the transition energy from injection to extraction energies. We also note that there is a systematic integer stopband at $a/b\approx1.93$, where $Q_x\approx2$. Beam motion at this condition would be unstable, and have a large horizontal betatron amplitude function. To avoid encountering stopbands, and to provide enough free space for extraction kickers, we choose $a=5.00$ m and $b=3.25$ m.

Figure 3 shows the betatron amplitude functions and the dispersion function of a superperiod for the lattice with $a=5.00$ m and $b=3.25$ m, a dipole edge angle of 8.5°, and a dipole length of 3.00 m.

C. Effect of dipole length and edge angle

Next we examine the effect of dipole length and its edge angle on the stability of betatron motion. The thick solid lines in Fig. 4 show the betatron tunes for dipole lengths of

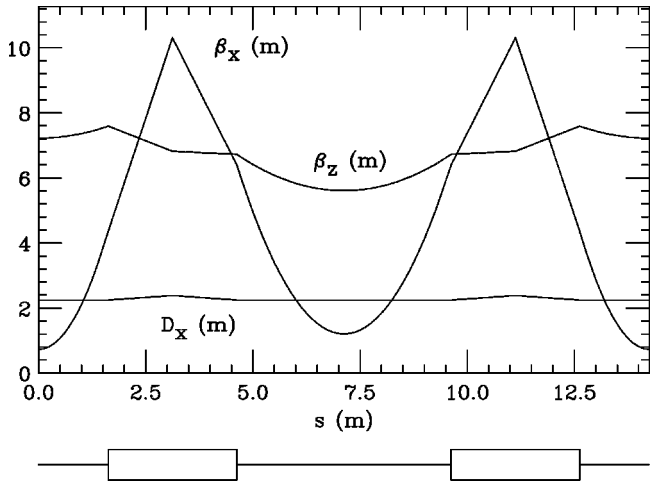

FIG. 3. Betatron amplitude functions for one superperiod. The CMS accelerator is made up of two superperiods.

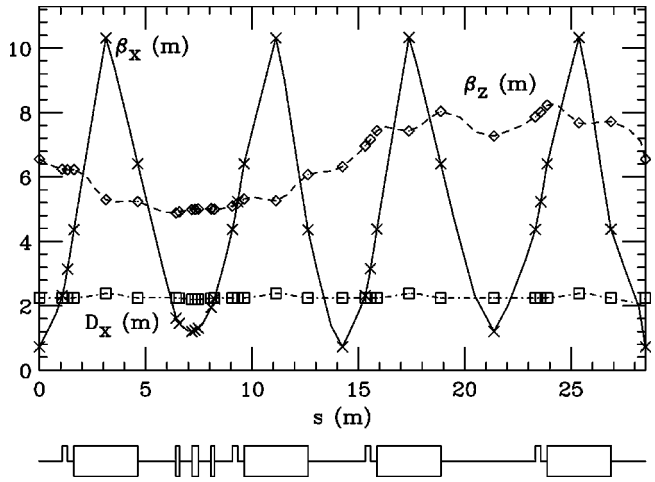

FIG. 5. Betatron amplitude functions for a complete accelerator including the effect of the chicane magnet system.

2.8, 2.9, 3.0, 3.1, and 3.2 m with edge angles of 7.0°, 7.5°, 8.0°, 8.5°, 9.0°, and 10°, respectively. The transition energy in all cases are above the maximum beam energy of 300 MeV.

Linear coupling and the third and the fourth order resonances are shown as dashed and dotted lines in Fig. 4. None of these resonances lines are systematic. On the other hand, the third order resonance shown as the dashed line is important for providing slow extraction for the beams at high energy. This is one of the reasons that we choose the dipole length to be 3.0 m with an edge angle of 8.5°. The resulting betatron amplitude functions are shown in Fig. 3.

D. Effects of the injection chicane system

For efficient beam injection, we consider a chicane magnet system with three dipoles. The H^- ion injected is stripped of its charge by a thin carbon foil at the end of the middle dipole. The location of the stripping foil must not inhibit the aperture to the circulating beam, i.e., the chicane kick angle $\theta_{ch} \approx 2\sqrt{\beta_x \epsilon_{95\%}}/L \approx 0.06$ rad, where L is the kicker arm from the middle of the last dipole to the location

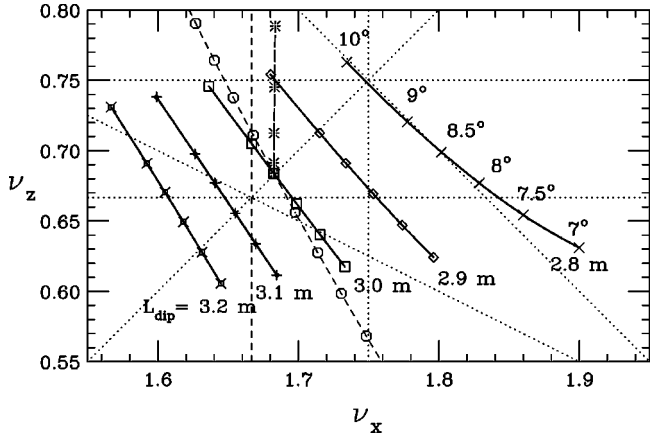

FIG. 4. Thick solid lines show the betatron tunes for dipole lengths from 2.8 to 3.2 m and edge angles from 7° to 10°. The effect of chicane magnets is shown as by asterisks and the effect of trim quadrupoles is shown by circles.

of the stripping foil. The asterisk in Fig. 4 shows the betatron tunes for chicane angles of 0, 0.025, 0.05, 0.075, and 0.100 rad, respectively.

The rectangular chicane magnets allow vertical focusing without much change in the horizontal tune and the transition energy. Vertical focusing increased the vertical betatron tune, and modified the vertical betatron amplitude function. Figure 5 shows the betatron amplitude functions with a chicane angle of $\theta_{ch} = 0.06$ rad. The two fold symmetry is broken where the vertical betatron function becomes smaller in the chicane area without much change in the horizontal betatron amplitude function. A smaller vertical betatron amplitude function at the stripper has the beneficial effect of decreasing the emittance growth rate due to multiple Coulomb scattering.

E. Effect of trim quadrupoles

A set of four trim quadrupoles can be used to make small adjustments to betatron tunes. We chose a position near each dipole, where $\langle \beta_x \rangle_t \approx 4.7$ m and $\langle \beta_z \rangle_t \approx 7.1$ m. The resulting betatron tune change is given approximately by

$$\Delta \nu_x = \frac{\langle \beta_x \rangle_t K_{1t} \ell_t}{4\pi B\rho}, \quad \Delta \nu_z = \frac{\langle \beta_z \rangle_t K_{1t} \ell_t}{4\pi B\rho} \tag{2}$$

for each trim quadrupole, where K_{1t} and ℓ_t are the quadrupole strength and the length of the trim quadrupole, respectively, and $B\rho$ is the beam rigidity. The effect of trim quads on the betatron tune is shown by the circle in Fig. 4. To change ν_x by 0.1, a quadrupole strength of 6.8 T/m for a quadrupole length of 0.25 m would be sufficient at a beam energy of 300 MeV. The trim quadrupoles can be used to move betatron tunes during slow extraction. They can also be programmed to compensate for the half-integer stopband during injection.

III. MAGNET SYSTEM

Assuming an admittance of 100 π mm mrad in both horizontal and vertical phase space with a momentum aperture of ± 0.005, we find that the full aperture of the magnet

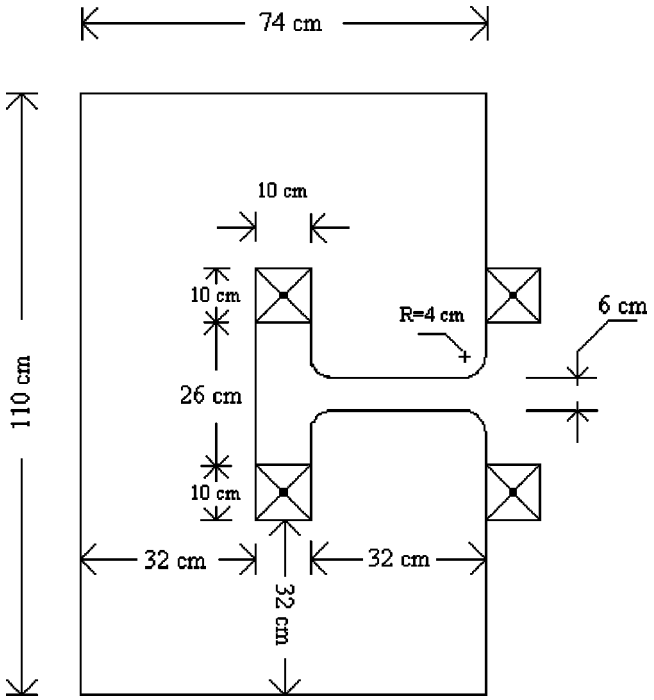

FIG. 6. Two-dimensional cross section of the magnet showing the geometry of the CMS *C*-type dipole magnet.

should be at least 66×56 mm^2 at injection with a full beam size of 30×25 mm^2 300 MeV. Figure 6 shows the cross section of a typical magnet design. The fractional magnetic field error as a function of the magnet aperture is shown in Fig. 7. The corresponding sextupole field strength is listed in Table II, where $B_2=\partial^2 B_z/\partial x^2|_{x=0,z=0}$ is the sextupole field strength. Using the sextupole field, we obtain the dynamical aperture shown in Fig. 8. Note that the dynamical aperture of the CMS is much larger than the physical aperture of the synchrotron.

Important issues for rapid cycling operations include aperture, eddy current, vacuum chamber design, and power supply.[8] For up to 10 Hz operation, the CIS magnet has a lamination thickness of 0.025 in. The magnets for the proton driver driver proposed at Fermilab at 15 Hz use a lamination

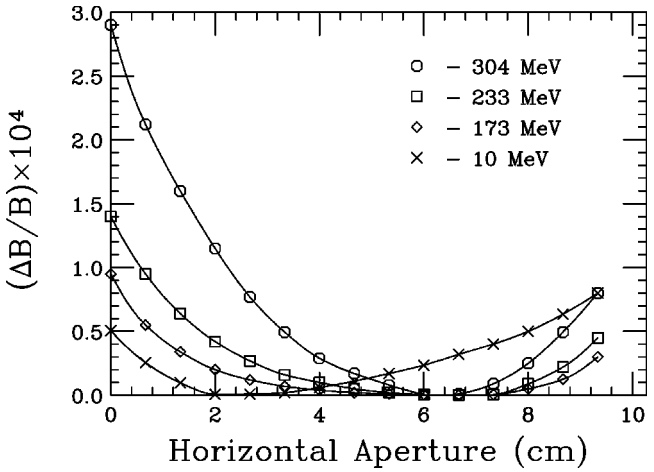

FIG. 7. Dipole field error the dipole aperture. The sextupole field strength derived is shown in Table II as a function of the corresponding beam energy.

TABLE II. Sextupole strength of the CMS magnets.

Energy (MeV)	$B_2/B\rho$ (1/m^3)
7.58	−0.058
17	−0.057
89	−0.051
143	−0.058
203	−0.065
261	−0.084
304	−0.121

thickness of 0.014 in. The magnet lamination of the CMS will depend on its primary purpose. A lamination thickness of 0.025 in. should be sufficient for all purposes. The lamination stacking can be shaped into blocks similar to those of CIS magnets. The end blocks are machined to attain a proper edge angle for vertical focusing.

The dipole and multipole fields induced by the eddy current on the vacuum chamber can also be important for rapid cycling synchrotrons.[9] The choices of vacuum chamber are (1) a thin vacuum chamber wall composed of higher resistivity materials, (2) a ceramic vacuum chamber, or (3) a chamber made of nonconductive composite materials plated with a thin layer of conducting material. Again, the choice depends on the main operational scheme for the CMS.

IV. THE rf SYSTEM

The revolution frequency of protons in the CMS covers a range of 1.28–6.86 MHz. Since the rf voltage required is $V_0 \sin\phi_s = 2\pi R\rho\dot{B}$, the cycling rate depends on the rf cavity voltage. At a nominal voltage of $V_0=500$ V, the maximum ramping rate is about 3 Hz for 300 MeV proton beam energy operation. The bucket height is about 0.65% at an injection energy of 7 MeV, and the invariant phase space area is about 0.1 eV s. A bunch stretcher to reduce the spread of momen-

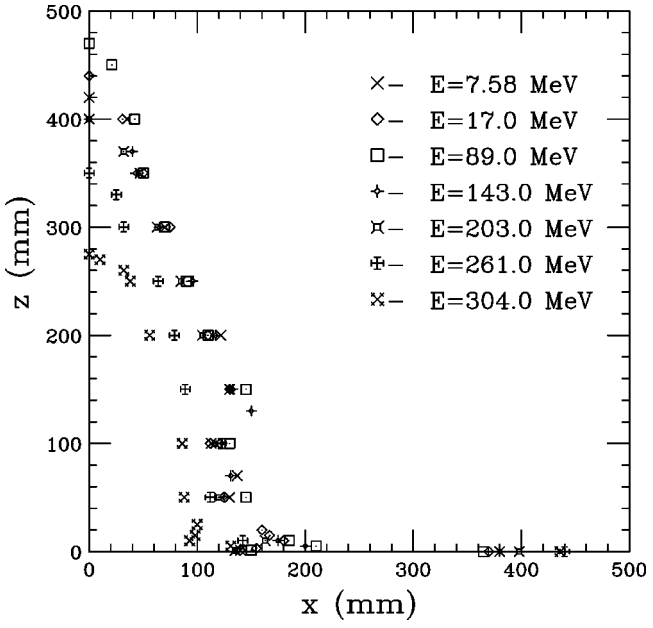

FIG. 8. Dynamical aperture of the CMS accelerator at various energies, where the sextupole field, derived from field strength calculations, is included in obtaining the dynamical aperture.

tum of the beam injected from the linac can be used to attain higher injection efficiency. For a fast ramping accelerator, beam chopping at the source can be used to alleviate the requirement of adiabatic capture, and can increase the injection efficiency.

The rf cavity must be ferrite loaded. Ferrite rings with quadrupole field bias have been successfully implemented in the Cooler Injector Synchrotron and the IUCF cooler.[10] To allow a fast tuning ratio starting around 1 MHz, a ferrite loaded coaxial structure is chosen for its minimum length and tuning potential. For example, the CIS cavity uses an assembly of 10 Phillips 8C12 ferrite rings to store virtually all the rf magnetic energy. A variable vacuum capacitor is used to reduce the number of ferrite rings required and hence the length of the cavity. Varying this loaded capacitance sets the working band of the cavity to as low as 0.5 MHz. Most ferrite bias tuned cavities have their biasing element exposed to the rf field. This is fine so long as the bias winding is no more than one to two turns. Otherwise the structure may resonate at various rf frequencies that can cause harm to rf operation. In order to obtain sufficient H field in amperes per turn, power supplies of hundreds to a few thousand amperes are required for a wider tuning range.

Biasing structures placed outside of the rf field no longer have this restriction and the magnetic windings can have as many turns as are practical. The CIS cavity has about 50 turns on each of the quadrupole tips. The quadrupole structure has the symmetry to cancel the field in the center of magnet where the beam passes through. A fairly compact variable power supply rated at 20 A maximum can achieve a 100:1 ratio of ferrite rf permeability change, resulting in a frequency sweep ratio of 10:1.

The ferrite rf loss generally increases with frequency. In conventional ferrite loaded cavities, the magnetic loop, where the driving rf power is fed, is coupled to a fixed percentage of the total cavity magnetic energy storage. This can lead to a significant change in impedance as seen from the rf driver and cause the rf power to largely be reflected. The problem is solved in the CIS cavity by varying this energy coupling ratio. This is accomplished by independent adjusting the strength of the quadrupole that biases the ferrite rings enclosed by the driving loop.

The ferrite rings are spaced in such a way as to make air cooling possible. Up to 2 kW of rf power can be handled this way with forced air cooling provided by the built-in high speed fan. The maximum gap voltage developed with full power excitation is around 1400 V. The cavity in this geometry, or similar in design, can be used in this CMS. For a rapid cycling operation, two CIS-like rf cavities may be needed fro the CMS.

V. FAST AND SLOW EXTRACTION SYSTEMS

The plan for a proton therapy treatment center may require both fast and slow beam extractions. At 300 MeV, the full size of the beam is about 15 mm at the point of extraction. For a fast beam extraction system, the kicker arm is $\sqrt{\beta_k \beta_s}\sin\phi_{12} \approx 3.2$ m. Thus the kicker angle required is 5 mrad, and the kicker field strength is about $B_{\text{kick}}\ell \approx 1.4 \times 10^{-2}$ T m at proton beam energy of 300 MeV. This can be achieved by a traveling wave or a magnetic kicker. A Lambertson septum can bring the beam onto the extraction channel.

Slow beam extraction is a useful method by which to attain high duty cycle operation of accelerator beams. The resonance strength of the third order slow extraction is given by

$$G_{3,0,5}e^{i\xi} = -\frac{\sqrt{2}}{24\pi}\int_{s_0}^{s_0+C}\frac{\beta_x^{3/2}B_2}{B\rho}e^{i[\chi(s)-(3\nu_x-5)\theta]}, \tag{3}$$

where s_0 is the location of the thin wire septum, $\chi(s) = \int_{s_0}^{s} ds/\beta_x(s)$ is the betatron phase advance, $\theta = (s - s_0)/R$, and B_2 is the sextupole strength. Here $G_{3,0,5}$ and ξ are the magnitude and phase of the third order resonance. Neglecting betatron detuning, the effective Hamiltonian in the action-angle (J_x, ϕ_x) variables is

$$H \approx \nu_x J + G_{3,0,5}J_x^{3/2}\cos(3\phi_x - 5\theta + \xi), \tag{4}$$

where $\theta = (s - s_0)/R$ serves as the time coordinate. With generating function $F_2 = (\phi_x - 5/3\theta)I_x$, where the new conjugate phase space coordinates are $I_x = J_x$ and $\psi_x = \phi_x - 5/3\theta$, the new Hamiltonian in the resonance rotating frame is

$$\tilde{H} = \delta I_x + G_{3,0,5}I_x^{3/2}\cos(3\psi_x + \chi), \tag{5}$$

where $\delta = \nu_x - 5/3 > 0$. The optimal phase for third order extraction is given by $\xi = -\pi/2$. The unstable fixed points (ufp) are located at

$$I_{x,\text{ufp}} = \frac{2\delta}{3G_{3,0,5}}, \quad \psi_{x,\text{ufp}} = \left(\frac{\pi}{2}, \frac{7\pi}{6}, \frac{11\pi}{6}\right). \tag{6}$$

A sextupole located at the straight section in front of the wire septum will provide the correct phase ξ for slow extraction.

VI. DISCUSSION OF IMPLEMENTATION

Applications of the accelerator described in this article range from isotope production and cancer proton beam surgery to versatile industrial applications. The intensity limit of 2.1×10^{11} protons per pulse arises essentially from the space charge consideration. This limit can be alleviated by a higher energy injector, a phase space painting scheme, or a proper stopband correction scheme using the trim quadrupoles. The fast extraction scheme can be implemented by a magnetic kicker or a traveling wave kicker. Slow extraction with high duty cycle can also be achieved by including sextupoles and trim quadrupoles. Using a flexible control system, this compact medical synchrotron can be a powerful source for medical applications. Details of the design of component subsystems depend on the main purpose for the compact synchrotron.

ACKNOWLEDGMENTS

The authors would like to thank Dr. George Berg and Dr. Alexander Pei for their help in the design of a prototype magnet and a possible rf system for CMS. This work was supported in part by grants from the U.S. Department of

Energy (US DOE) Grant No. DE-FG0292ER40747, and from the National Science Foundation, Grant No. PHY-0140251.

[1] See, for example, G. Coutrakon and J. M. Slater, *Proceedings of the Particle Accelerator Conference* (IEEE, Piscataway, NJ, 1999), p. 11.
[2] See, for example, J. Alonso, *Proceedings of the 2000 European Particle Accelerator Conference* (EPAC, 2000), p. 235.
[3] K. Hiramoto *et al.*, *Proceedings of the 1997 Particle Accelerator Conference* (IEEE, Piscataway, NJ, 1997), p. 3813; A. Yamaguchi *et al.*, *ibid.*, p. 3828; A. Morita *et al.*, *Proceedings of the 1999 Particle Accelerator Conference* (IEEE, Piscataway, NJ, 1999), p. 2528; K. Endo *et al.*, *Proceedings of the 2000 European Particle Accelerator Conference* (EPAC, 2000), p. 2515.
[4] X. Kang, Ph.D. thesis, Indiana University, Bloomington, IN, 1998 (unpublished).
[5] In general, the beam intensity and emittance are determined by the space charge effect, where the half integer resonance can cause beam envelope oscillations, dilution of beam emittance, and beam loss (after Ref. 6). The choice of beam emittance is based on the space charge tune shift limit, where the incoherent space charge tune shift serves as a scaling factor.
[6] See, for example, S. Y. Lee, *Accelerator Physics* (World Scientific, Singapore, 1999).
[7] The energy and types of injector (RFQ/DTL vs cyclotron) can be further evaluated for possibile integration of nuclear medicine into the integrated medical complex.
[8] See, for example, *The Proton Driver Design Study*, edited by W. Chou, C. Ankenbrandt, and E. Malamud (Fermilab TM-2136, 2001).
[9] See, for example, S. Y. Lee, Nucl. Instrum. Methods Phys. Res. A **300**, 151 (1990).
[10] A. Pei *et al.*, *Proceedings of the IEEE Particle Accelerator Conference* (IEEE, Piscataway, NJ, 1995), pp. 1705, 1708; *ibid.* (IEEE, Piscataway, NJ, 1997), p. 2968.